Non-Gaussian rotational diffusion in heterogeneous media

Heejin Jeon, Hyun Woo Cho, Jeongmin Kim, and Bong June Sung
Department of Chemistry, Sogang University, Seoul 121-742, Republic of Korea
(Received 12 May 2014; revised manuscript received 11 September 2014; published 3 October 2014)

We employ a simple model for rotational diffusivity D_R of dumbbells in porous media in order to study spatially heterogeneous and non-Gaussian dynamics at Fickian time scales. We obtain the distribution $P(D_R)$ of D_R's of single dumbbells for both ergodic and nonergodic systems. When a pore percolating network disappears beyond the pore percolation transition and the rotational dynamics becomes nonergodic, each single dumbbell undergoes Gaussian rotational dynamics but with different D_R, which depends solely on the local pore structure. We also construct a map of heterogeneous dynamic regions and illustrate that such seemingly Fickian but non-Gaussian dynamics could be understood as the linear combination of the Gaussian rotational displacement distribution functions of each dumbbell. With a percolating pore network, the rotational dynamics becomes ergodic, and $P(D_R)$ is a δ function at the average value of D_R.

DOI: 10.1103/PhysRevE.90.042105 PACS number(s): 05.40.−a, 82.70.−y, 66.30.hh, 45.20.dc

I. INTRODUCTION

The dynamics of single molecules is spatially heterogeneous in complex systems such as glasses and cells [1–9]. For example, band 3 molecules in human red blood cells rotate with a broad range of rotational relaxation times τ [10–12]. τ is smaller than 250 μs for about 20% of band 3 molecules, whereas $\tau \sim 1$ ms for most cases. A small fraction of band 3 molecules is even rotationally immobile. Such heterogeneous systems consist of regions of different dynamics: fast, slow, and intermediate regions [2,6,9,13]. The characteristic size of each region in glasses, for example, is about a few nanometers, and the dynamics varies by several orders of magnitude [2]. Recent experiments and simulations showed that when the rotational correlation function $U(t)$ was averaged over many molecules in different regions, $U(t)$ was stretched exponential, i.e., $U(t) \sim \exp[-(t/\tau)^{\beta}]$ with $0 < \beta < 1$ [2,9,14,15]. The stretched-exponential form of $U(t)$ is considered a clear indication of dynamic heterogeneity [2,9,16–21].

Such dynamic heterogeneity has been described in terms of the distribution τ or the distribution $P(D)$ of diffusion coefficients D [22–25]. It is, however, usually formidable to obtain $P(D)$: (1) in ergodic systems there is no distribution of D, i.e., $P(D)$ reaches a δ function after sufficient time averaging, and (2) in nonergodic systems such as glasses the diffusion is usually too slow to estimate $P(D)$. Therefore, it should be an issue of importance to develop a model system, obtain $P(D)$ for both ergodic and nonergodic systems, and investigate the notion of dynamic heterogeneity systematically. In this work, we consider a model system where a dumbbell is located in porous media with or without a percolating pore network. Without a percolating pore network, no dumbbell can escape from its own region, and its dynamics is nonergodic, depending solely on the structure of the local region [26]. On the other hand, when a percolating pore network exists, each dumbbell travels over many pores, and the dynamics becomes ergodic.

Recent single-molecule experiments in entangled actin networks, gels, and colloidal suspensions revealed that while the dynamics was Fickian, i.e., the mean-square displacement $W(t)$ was linear with time t, the displacement distribution function [or the van Hove correlation function, $G_s(r,t)$] was non-Gaussian instead of being Gaussian [24,25,27–31]. Because $W(t) \sim t$ indicates that molecules would undergo Brownian diffusion at given time scales, the Gaussian form of $G_s(r,t)$ is usually expected. However, there have been several reports of such a seemingly Fickian but non-Gaussian dynamics in complex systems [23–25,27–31], and how the non-Gaussian $G_s(r,t)$ emerges still remains elusive. Non-Gaussian $G_s(r,t)$ has been interpreted as a linear combination of the Gaussian displacement distribution functions $g(r,t|D)$ of each single molecule, i.e., $G_s(r,t) = \int P(D)g(r,t|D)dD$. However, it is still a difficult task to verify the interpretation because for ergodic systems $P(D)$ becomes a δ function and for nonergodic systems it is daunting to estimate $P(D)$. In this work, we obtain $P(D)$ for both ergodic and nonergodic systems and illustrate that such non-Gaussian dynamics should result from the linear combination of Gaussian displacement distributions of single molecules. We investigate the rotational diffusion of dumbbells in porous media around a pore percolation transition. When a dumbbell is confined in its own local region with no pore percolating network, the angular displacement distribution function $g(\theta,t|D_R)$ (the van Hove function for the rotational motion) of each dumbbell is Gaussian. But the rotational diffusion coefficient D_R of each dumbbell differs for different dumbbells depending on the structure of the local region. When $g(\theta,t|D_R)$'s are averaged over all dumbbells, the averaged angular displacement distribution function $G_s(\theta,t)$ is exponential instead of being Gaussian.

Recent theoretical and simulation studies by Fierro *et al.* [23,32] showed that the dynamics of permanent gels was also non-Gaussian at Fickian time scales and verified systematically that such non-Gaussian dynamics could be understood as a linear combination of the Gaussian displacement distribution functions of different values of D_s, where D_s is the diffusion coefficient of cluster size s of permanent gels. By employing the percolation theory and assuming the relation between D_s and s, they proposed a quantitative theory to explain the complex dynamic behavior of gels in terms of $P(D_s)$ and compared the theory to their simulation results.

There have been various relevant experiments for the rotational diffusion in complex systems [33–37]. For example, in recent single-molecule experiments, the wobbling dynamics

of single molecules in silica mesopores was investigated [33,34]. Some single molecules traveled between different mesopores and showed different dichroism emission in different mesopores depending on the pore structure. This suggests that the rotational dynamics would be heterogeneous due to the structural difference in mesopores. Another recent experiment was also performed to investigate the rotational dynamics of nanodoublers (noncentrosymmetric crystalline particles) in living cells [35]. In the experiment, $P(D_R)$ was obtained and the spatial map of D_R was also constructed, which illustrated the dynamic heterogeneity of rotational diffusion in living cells and is consistent with our simulation results.

In porous media molecules may diffuse translationally only when a pore percolating network exists [7,38–43]. When the matrix density ϕ is smaller than a critical value ϕ_c, a pore percolating network exists, and $W(t) \sim t$ at long times. At the percolation transition ($\phi = \phi_c$), $W(t) \sim t^{\alpha}$ at all time scales with $\alpha < 1$, i.e., the translational diffusion is subdiffusive [44–46]. For $\phi > \phi_c$, the pore percolating network disappears. Because all molecules are confined in local pores for $\phi > \phi_c$, molecules cannot diffuse, and $W(t)$ approaches a plateau. Such an interesting translational diffusion in porous media is very similar to the protein diffusion in cell membranes [1,3,7,41,47]. Porous media, therefore, have been employed as a model system for cell membranes. Since the translational diffusivity disappears but molecules still rotate for $\phi > \phi_c$, it would not be surprising if the translational motion of molecules were to separate from the rotational motion. But we illustrate in this work that a certain mode of rotational relaxation should accompany the translational motion of molecules even for $\phi > \phi_c$, which should account for the anomalous oscillatory relaxation of $G_s(\theta,t)$ observed in our simulations.

The rest of this paper is organized as follows. Our model and simulation details are described in Sec. II. Simulation results are presented and discussed in Sec. III. Finally, a summary and conclusions are presented in Sec. IV.

II. MODEL AND METHODS

Porous media are modeled as a set of monodisperse hard disks (matrix particles) that are randomly distributed and quenched in two dimensions. The diameter σ of hard disks is the unit length in our simulations. A dumbbell is modeled as a dimer of hard disks of the same diameter σ. The bond distance of a dumbbell is allowed to fluctuate from 0.95 to 1.05. In order to obtain initial configurations, we place matrix particles sequentially at random positions. The position is accepted if the matrix particle does not overlap with preexisting particles, and otherwise, it is discarded. The procedure is repeated until a desired matrix density (or area fraction) ϕ ($\equiv \pi\sigma^2 N_m/4L^2$, where N_m is the number of matrix particles and L is the simulation cell dimension) is obtained. L ranges from 50 to 100, and periodic boundary conditions are applied in all directions. Once the configurations of porous media are obtained, dumbbells are placed at random positions. No overlap between dumbbells and other particles is allowed. The area fraction ($\phi_f \equiv 2\pi\sigma^2 N_f/4L^2$, where N_f is the number of dumbbells) of dumbbells is fixed at 0.01.

Ten initial configurations are generated for each ϕ and are used to ensemble average observables. Because of quenched disorder inherent in porous media, double ensemble averaging should be carried out; that is, an observable needs to be averaged first over all dumbbells in each realization of porous media and then over many realizations of porous media. The system is evolved via a discontinuous molecular dynamics (DMD) simulation that employs an event-driven algorithm [48]. For each successive collision between two particles, the momenta and positions of dumbbells are updated based on the conservation laws of energy and momentum. When a pore percolating network exists, the system is equilibrated until the mean-square displacement of dumbbells is at least larger than $50\sigma^2$. In the absence of a pore percolating network, the system is equilibrated until the mean-square angular displacement is at least larger than 50. In both cases, the time correlation function $U(t)$ of the director of a dumbbell decays to zero, except in the case of the largest value of $\phi = 0.4$.

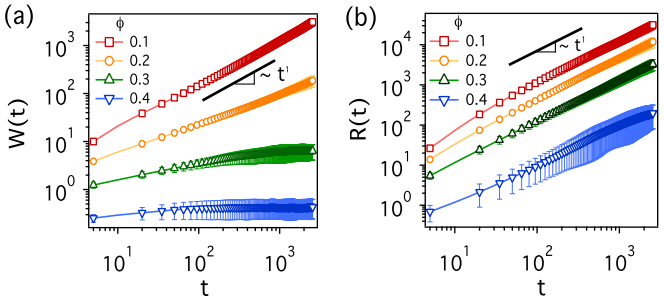

FIG. 1. (Color online) Simulation results for (a) the mean-square displacement $W(t)$ of the center of mass of the dumbbells and (b) the mean-square angular displacement $R(t)$.

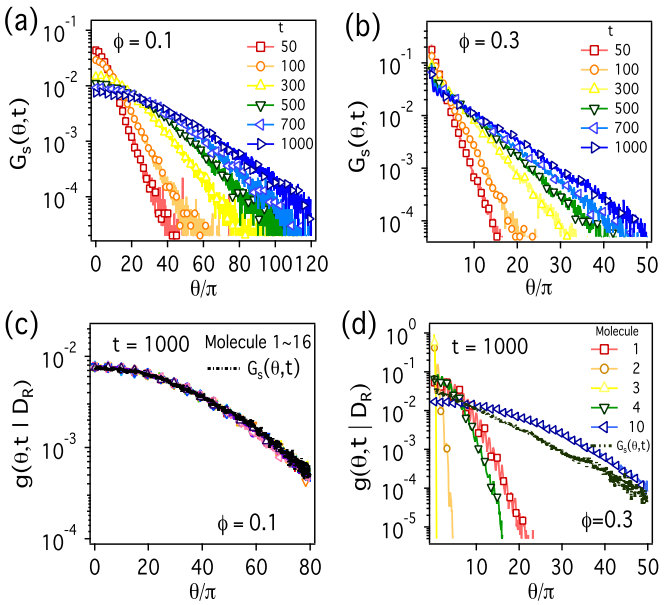

FIG. 2. (Color online) Simulation results for angular displacement distribution functions $G_s(\theta,t)$ averaged over all dumbbells for (a) $\phi = 0.1$ and (b) $\phi = 0.3$. Time-averaged angular displacement distribution functions $g(\theta,t|D_R)$ of individual dumbbells for (c) $\phi = 0.1$ and (d) $\phi = 0.3$.

III. RESULTS AND DISCUSSION

The pore percolation threshold area fraction ϕ_c depends on the size of the tracers and the polydispersity of matrix particles [41–43]. It is well known that $\phi_c \approx 0.22$ when the matrix particles are monodisperse and the size of the tracer is identical to that of the matrix particles, as in this study. When $\phi < \phi_c$, a pore percolating network should exist. On the other hand, for $\phi > \phi_c$, the pore percolating network disappears, and all dumbbells are confined in local regions. Figure 1(a) depicts the mean-square displacements $[W(t) \equiv \langle|\vec{r}(t) - \vec{r}(0)|^2\rangle]$. $\vec{r}(t)$ denotes the position vector of the center of mass of a dumbbell at time t, and $\langle\cdots\rangle$ represents an ensemble average. For $\phi = 0.1$, $W(t) \sim t$ in our simulation times. For $\phi > \phi_c = 0.22$, $W(t)$ reaches a plateau, indicating that all dumbbells are confined in local pores. For $\phi = 0.2$, dumbbells show subdiffusive behavior in our simulation times. But dumbbells are expected to enter the Brownian regime for longer times with $W(t) \sim t$.

The rotational diffusion of dumbbells is Fickian for all values of ϕ in our simulations. We estimate the mean-square angular displacements $[R(t) \equiv \langle|\theta(t) - \theta(0)|^2\rangle]$. $\theta(t)$ is the angle of a dumbbell with respect to a reference axis at time t. Note that the unit of θ in this study is radians and that the rotational motion in two dimensions corresponds to the one-dimensional walk along the θ axis. $R(t) \sim t$ at large times for all values of ϕ in our study, as depicted in Fig. 1(b). This indicates that even when dumbbells are confined in local pores with no pore percolating network and are not able to diffuse, they are still allowed to rotate.

The rotational displacement distribution function averaged over all dumbbells $[G_s(\theta,t) \equiv \langle\delta\{\vec{\theta} - [\theta(t) - \theta(0)]\}\rangle]$ is Gaussian for small ϕ, as expected. For $\phi = 0.1$, dumbbells undergo Brownian rotational motion; thus, $R(t) \sim t$ and $G_s(\theta,t)$

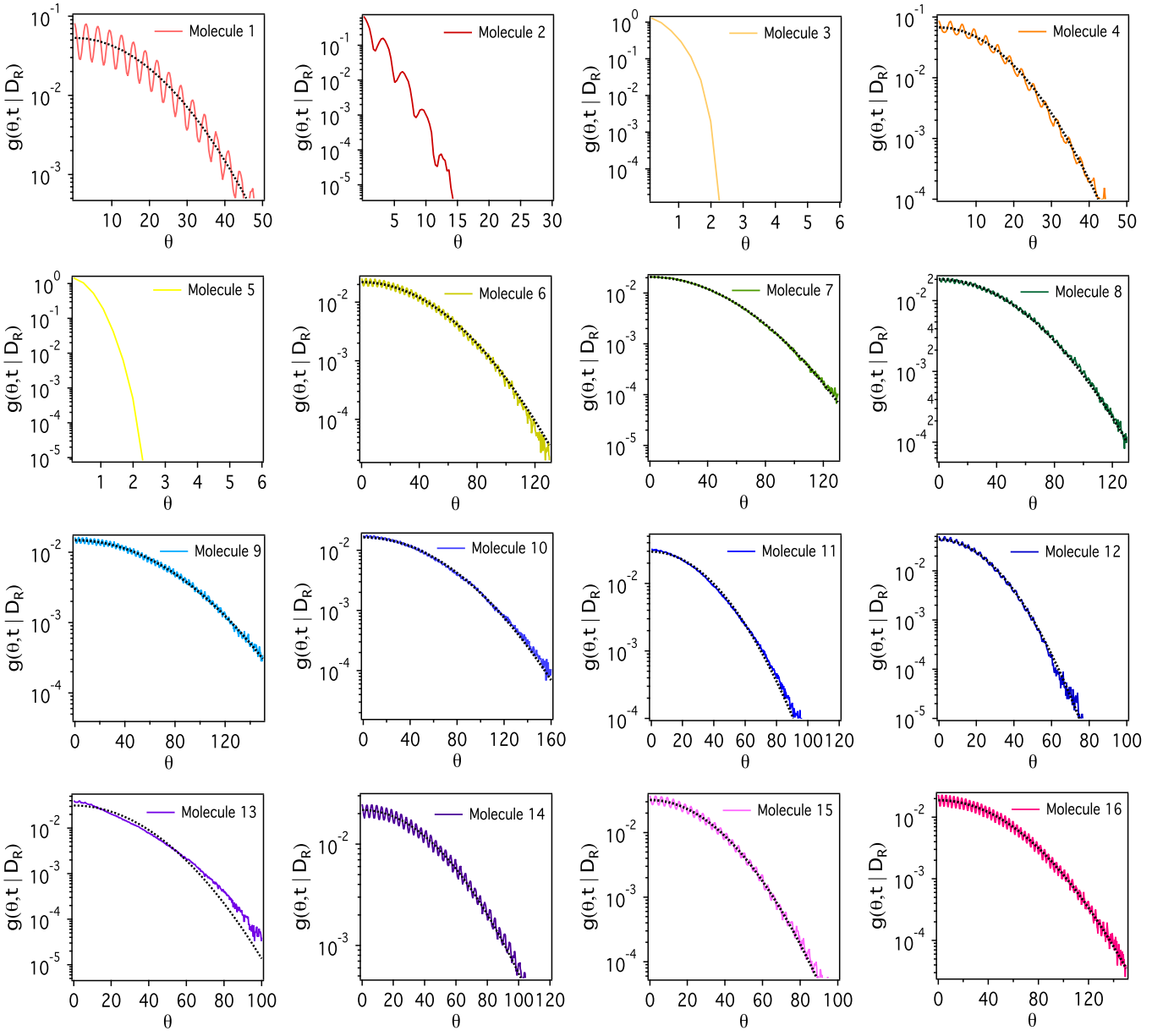

FIG. 3. (Color online) $g(\theta,t|D_R)$ for individual dumbbells as a function of θ for $t = 1000$ and $\phi = 0.3$.

is Gaussian at large times [Fig. 2(a)]. The time-averaged rotational displacement distribution function $g(\theta,t|D_R)$ of individual dumbbells is also all Gaussian, with an identical rotational diffusion coefficient D_R.

For $\phi = 0.3$ beyond the pore percolation transition, the ensemble-averaged $G_s(\theta,t)$ is exponential at large θ, as depicted in Fig. 2(b). Note that $R(t) \sim t$ for $\phi = 0.3$, which indicates that the rotational dynamics should be Fickian and that Gaussian $G_s(\theta,t)$ would be expected. However, $G_s(\theta,t)$ is exponential even at large times. Such a seemingly Fickian but non-Gaussian dynamics was also observed in heterogeneous systems such as entangled actin networks, gels, and colloidal mixtures [24,25,27–31]. In those systems, translational displacement distribution functions $G_s(r,t)$ were Gaussian at short r and non-Gaussian at large r while $W(t) \sim t$.

Previous studies [25,27] proposed that such a non-Gaussian ensemble-averaged $G_s(\theta,t)$ at Fickian time scales would be interpreted as a linear combination of Gaussian $g(\theta,t|D_R)$'s of single molecules that rotate with different rotational diffusion coefficients D_R, i.e.,

$$G_s(\theta,t) = \int P(D_R) g(\theta,t|D_R) dD_R, \qquad (1)$$

where $P(D_R)$ is the effective distribution function of rotational diffusion coefficients, representing the spatial heterogeneity of systems. If a molecule were allowed to sample all regions of different dynamics, the molecule might rotate with a different *transient* D_R in a given local region, but the molecule would travel all regions of different dynamics eventually. Then, $G_s(\theta,t)$ and $g(\theta,t|D_R)$ would be identical to each other [Fig. 2(c)]. In such a case $P(D_R)$ does not necessarily mean that there should be a distribution of diffusion coefficients. However, determining whether the trajectory of a single molecule would be sufficiently long and/or how many regions a single molecule would have sampled would be difficult tasks in both experiments and simulations.

In our systems for $\phi > \phi_c$, dumbbells are confined in their own regions and are not allowed to sample other regions due to the absence of pore percolating networks. $G_s(\theta,t)$ is therefore different from $g(\theta,t|D_R)$ for a single dumbbell. A single dumbbell rotates with different rotational diffusion coefficients D_R, and $g(\theta,t|D_R)$ for each single dumbbell is Gaussian (Fig. 3). Figure 2(d) depicts time-averaged $g(\theta,t|D_R)$'s of five representative dumbbells at $t = 1000$. While some dumbbells (molecule 2) rotate slowly, others may rotate quickly with large D_R. Figure 3 depicts $g(\theta,t|D_R)$'s of 16 individual dumbbells. All of 16 $g(\theta,t|D_R)$'s are Gaussian functions of θ for $t = 1000$ and $\phi = 0.3$ even though the rotational diffusion coefficient D_R differs for different dumbbells. When all $g(\theta,t|D_R)$'s are averaged over all dumbbells and media configurations, the ensemble-averaged $G_s(\theta,t)$ becomes non-Gaussian and exponential, as depicted in Fig. 2(d).

We also scale $g(\theta,t|D_R)$ by D_R of each dumbbell for $\phi = 0.3$ (Fig. S1 in the Supplemental Material [49]). For all dumbbells except rotationally immobile ones, the scaled $g(\theta,t|D_R)$'s overlap well with one another, implying that $g(\theta,t|D_R)$'s are all Gaussian but have different values of D_R. Figure 4(a) depicts the distribution of D_R for different values of ϕ. When there are percolating pore networks ($\phi = 0.1$ to 0.2), $P(D_R)$ reaches a δ function at the average value ($\langle D_R \rangle$)

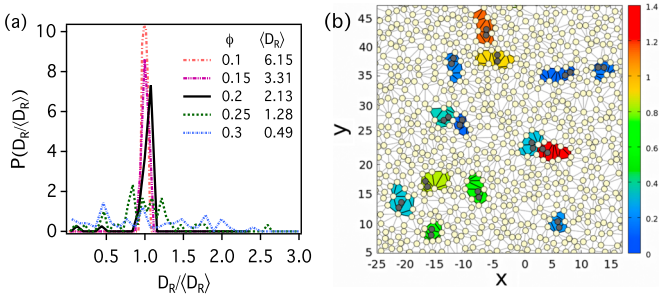

FIG. 4. (Color online) (a) The scaled distribution of D_R. $\langle D_R \rangle$ denotes the averaged value of D_R. (b) A simulation snapshot of dumbbells with Delaunay triangles. Light yellow (light gray) and dark gray circles represent matrix particles and dumbbells, respectively. Solid lines are the edges of Delaunay triangles. Shaded (colored online) triangles are regions that contain dumbbells. The value of D_R of the dumbbell in each shaded triangle is presented by the area color according to the bar on the right.

of D_R. When the percolating pore network vanishes and the dumbbell dynamics becomes nonergodic for $\phi = 0.25$ and 0.3, broad distribution functions [$P(D_R)$] of D_R are observed.

Because each dumbbell is isolated in its own region and is not allowed to sample over many regions, the rotational diffusion coefficient D_R tells us how fast the dynamics would be in each region. Figure 4(b) shows the map of local regions of fast, slow, and intermediate dynamics with Delaunay triangles [50] embedded for $\phi = 0.3$. Solid lines depict the edges of Delaunay triangles whose vertices are located on the center of matrix particles [yellow (light gray) circles]. Delaunay triangles with the same color construct a local region for a single dumbbell (dark gray circles). Fourteen dumbbells are shown in Fig. 4(b). Shaded (colored online) triangles in Fig. 4(b) are regions where dumbbells are confined. The values of D_R's of the dumbbells vary among dumbbells by orders of magnitude, and are represented by the colors of the regions according to the bar on the right. Figure 4(b) illustrates clearly that the system consists of regions of different dynamics: fast, slow, and intermediate regions. The map of local regions corresponds conceptually to the schematic illustration of regions of spatially heterogeneous dynamics for glasses [2]. A recent experiment was carried out for the rotational diffusion of nanodoublers in living cells. A spatial map of D_R's was constructed for living cells and is qualitatively identical to our map.

The rotational diffusion of a dumbbell is sensitive to the local structure of a pore. We construct a set of rectangular pores that consist of hard disks, and we place a dumbbell in the rectangular pore and perform discontinuous molecular dynamics simulations. The width w and height h of rectangular pores are changed from 2σ to 4σ. For example, if a dumbbell is located in a rectangular pore of $w = 4$ and $h = 1$, there is not much free area for the dumbbell to rotate in. $g(\theta,t|D_R)$ hardly propagates with time for $(w,h) = (4,1)$, indicating that dumbbells in the pore are rotationally immobile. On the other hand, in the case of rectangular pores of $(w,h) = (2,2)$ and $(4,3)$, $g(\theta,t|D_R)$'s are Gaussian with relatively large D_R (Fig. S2 in the Supplemental Material [49]). More interestingly, for $(w,h) = (4,2)$, $g(\theta,t|D_R)$ shows an oscillatory behavior even

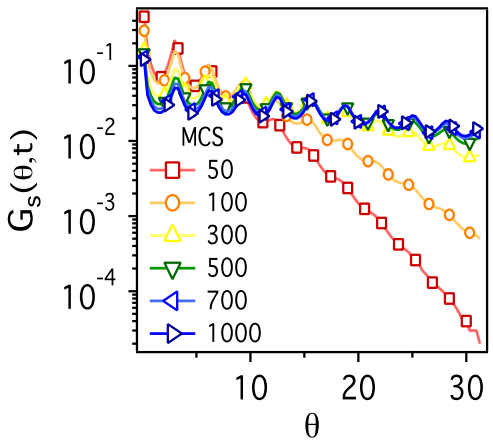

FIG. 5. (Color online) Monte Carlo (MC) simulation results for the angular displacement distribution functions $G_s(\theta,t)$ averaged over all dumbbells for $\phi = 0.3$. MCS denotes the number of Monte Carlo steps and is a time unit in MC simulations.

at $t = 1000$, which is not observed for $(w,h) = (2,2)$ and $(4,3)$. We find from the trajectories of the dumbbells that $g(\theta,t|D_R)$ becomes oscillatory only when dumbbells are allowed to carry out translational motion in one direction for anisotropic pores with sufficiently small height (or width).

We also perform Monte Carlo simulations for media configurations that were used in DMD simulations (Fig. 5). The oscillatory behavior of $G_s(\theta,t)$ is still observed for MC simulations for various times. This implies that the oscillatory behavior should not result from the ballistic nature of DMD simulations. Considering that the oscillatory behavior of $g(\theta,t|D_R)$ of an individual dumbbell is sensitive to the structure of a local pore, we believe that the oscillatory behavior should originate from the anisotropic structure of local pores in porous media.

The time correlation function $U(t)$ of a director of a dumbbell is also calculated, i.e., $U(t) \equiv \langle \vec{R}(t) \cdot \vec{R}(0) \rangle$, where $\vec{R}(t)$ is the director, or the normalized end-to-end vector, of the dumbbell at time t. According to the Boltzmann equation and a kinetic model [51], $U(t) = B(t) + \frac{1}{\tau}\int_0^t ds B(s)U(t-s)$, where $B(t) = \exp(-\frac{k_BT}{2I}t^2 - t/\tau)$ and the reduced mass $I = 1/2$ and $k_BT = 1$ in this study. When the interaction of dumbbells with matrix particles is scarce, $\tau \to \infty$ and $U(t) \to B(t) = \exp(-t^2)$. In the case of $\phi = 0.1$ and 0.2, dumbbells may rotate even without colliding with matrix particles, τ is quite large, and $U(t)$ decays before $R(t)$ reaches a Fickian time regime, i.e., $R(t) \sim t$. Therefore, $U(t)$ decays faster than an exponential decay. However, the rotational dynamics of dumbbells is homogeneous; that is, $U(t)$'s of single dumbbells are identical to one another [Fig. 6(b)]. As expected, $U(t)$ decays more slowly with an increase in ϕ. For $\phi = 0.4$, the local pores are so small that there are many rotationally immobile dumbbells, and $U(t)$ hardly decays in our simulation times [Fig. 6(a)]. For $\phi = 0.3$, the time-averaged $U(t)$'s of individual dumbbells are categorized into three types: (1) most dumbbells rotate with exponential relaxation functions, but the relaxation times are different, (2) a few dumbbells are rotationally immobile, and (3) the time-averaged $U(t)$ of some dumbbells are stretched exponential themselves [Fig. 6(c) and Fig. S3 in the Supplemental Material [49]]. For the last case, a single dumbbell is confined in a relatively large tortuous pore such that the pore may consist of more than one local region itself, and the dumbbell may undergo rotational hopping motions in the pore [52]. When averaging the time-averaged $U(t)$'s over all molecules in the three types, the ensemble-averaged $U(t)$ is not exponential but stretched exponential with $\beta = 0.244$, which indicates that dumbbells show both spatial and temporal heterogeneous dynamics in dense porous media.

In porous media structural heterogeneity exists due to the quenched disorder, which is different from the case for supercooled liquids and glasses. In porous media molecules in different pores experience different local structure, which results in the spatially heterogeneous dynamics. Therefore, even though our model of dumbbells in porous media allows us to estimate $P(D_R)$ and explain non-Gaussian dynamics for nonergodic systems, there is a caveat that it is still an important issue to investigate the non-Gaussian dynamics and $P(D)$ in glasses and supercooled liquids. However, note that the structural heterogeneity in porous media is significant even when a percolating pore network exists, for which dumbbells show anomalous translational diffusion, i.e., $W(t) \sim t^\alpha$ with $\alpha < 1$ for a few orders of magnitude of time [Fig. 1(a)]. However, the rotational dynamics of dumbbells is still homogeneous for $\phi < \phi_c$, and $P(D_R)$ is a δ function [Fig. 4(a)]. The rotational dynamics becomes heterogeneous only when a percolating pore network disappears for $\phi > \phi_c$. This implies that even though the structural heterogeneity plays an important role in the heterogeneous dynamics of dumbbells, the percolation transition and the ergodicity breakage are also critical to the dynamic heterogeneity of dumbbells.

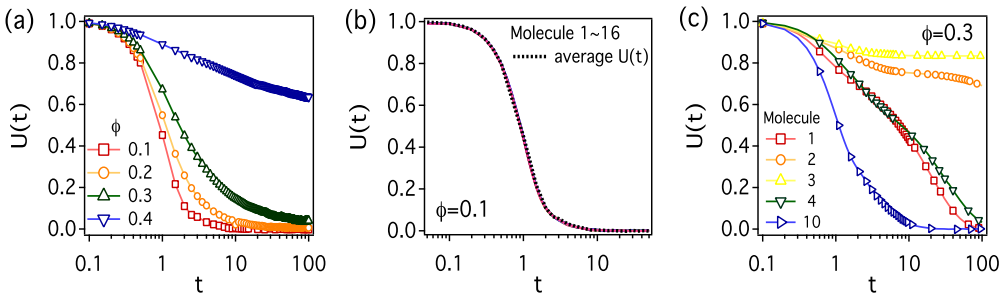

FIG. 6. (Color online) (a) Time correlation function $U(t)$ averaged over all dumbbells for each value of ϕ from 0.1 to 0.4. $U(t)$'s of representative individual dumbbells for (b) $\phi = 0.1$ and (c) $\phi = 0.3$.

IV. SUMMARY

We perform discontinuous molecular dynamics simulations for dumbbells in porous media near the pore percolation transition. For all values of ϕ in our simulations, the mean-square angular displacement $R(t)$ is linear with time; that is, the rotational dynamics is Fickian, even without pore percolating networks. However, when the pore percolating network disappears, dumbbells are isolated in local regions, and the rotational motion of each dumbbell becomes sensitive to the local pore structure. Even though the rotational dynamics is Fickian, the van Hove rotational correlation function $G_s(\theta,t)$ is non-Gaussian. More interesting is that the time-averaged rotational displacement distribution $g(\theta,t|D_R)$ of each dumbbell is Gaussian with different values of D_R. This clearly shows that when Gaussian $g(\theta,t|D_R)$'s are averaged over all dumbbells, the ensemble-averaged $G_s(\theta,t)$ becomes non-Gaussian. We obtain $P(D_R)$'s for both ergodic and nonergodic systems and show that non-Gaussian dynamics can be interpreted as the linear combination of the Gaussian displacement distribution functions of single molecules of different D_R.

ACKNOWLEDGMENTS

The authors would like to thank K. Paeng for valuable comments. This research was supported by the Basic Science Research Program through the National Research Foundation of Korea (NRF) funded by the Ministry of Education, Science and Technology (Grant No. NRF-2013R1A1A2009972).

[1] M. J. Saxton and K. Jacobson, Annu. Rev. Biophys. Biomol. Struct. **26**, 373 (1997).
[2] M. D. Ediger, Annu. Rev. Phys. Chem. **51**, 99 (2000).
[3] A. Kusumi, C. Nakada, K. Ritchie, K. Murase, K. Suzuki, H. Murakoshi, R. S. Kasai, J. Kondo, and T. Fujiwara, Annu. Rev. Biophys. Biomol. Struct. **34**, 351 (2005).
[4] S.-H. Chong and W. Kob, Phys. Rev. Lett. **102**, 025702 (2009).
[5] K. V. Edmond, M. T. Elsesser, G. L. Hunter, D. J. Pine, and E. R. Weeks, Proc. Natl. Acad. Sci. USA **109**, 17891 (2012).
[6] M. D. Ediger and P. Harrowell, J. Chem. Phys. **137**, 080901 (2012).
[7] F. Höfling and T. Franosch, Rep. Prog. Phys. **76**, 046602 (2013).
[8] B. R. Parry, I. V. Surovtsev, M. T. Cabeen, C. S. O'Hern, E. R. Dufresne, and C. Jacobs-Wagner, Cell **156**, 183 (2014).
[9] K. Paeng and L. J. Kaufman, Chem. Soc. Rev. **43**, 977 (2014).
[10] R. H. Austin, S. S. Chan, and T. M. Jovin, Proc. Natl. Acad. Sci. USA **76**, 5650 (1979).
[11] J. D. Corbett, P. Agre, J. Palek, and D. E. Golan, J. Clin. Invest. **94**, 683 (1994).
[12] F. L. Brown, D. M. Leitner, J. A. McCammon, and K. R. Wilson, Biophys. J. **78**, 2257 (2000).
[13] S. R. Becker, P. H. Poole, and F. W. Starr, Phys. Rev. Lett. **97**, 055901 (2006).
[14] C.-Y. J. Wei, Y. H. Kim, R. K. Darst, P. J. Rossky, and D. A. Vanden Bout, Phys. Rev. Lett. **95**, 173001 (2005).
[15] H.-N. Lee, K. Paeng, S. Swallen, and M. D. Ediger, Science **323**, 231 (2009).
[16] A. Toelle and H. Sillescu, Langmuir **10**, 4420 (1994).
[17] J. Kanetakis, A. Tölle, and H. Sillescu, Phys. Rev. E **55**, 3006 (1997).
[18] G. Hinze, G. Diezemann, and T. Basché, Phys. Rev. Lett. **93**, 203001 (2004).
[19] C. De Michele, R. Schilling, and F. Sciortino, Phys. Rev. Lett. **98**, 265702 (2007).
[20] S. A. Mackowiak and L. J. Kaufman, J. Phys. Chem. Lett. **2**, 438 (2011).
[21] A. A. Milischuk and B. M. Ladanyi, J. Chem. Phys. **135**, 174709 (2011).
[22] S. Sengupta and S. Karmakar, J. Chem. Phys. **140**, 224505 (2014).
[23] A. Fierro, T. Abete, and A. Coniglio, J. Chem. Phys. **131**, 194906 (2009).
[24] P. I. Hurtado, L. Berthier, and W. Kob, Phys. Rev. Lett. **98**, 135503 (2007).
[25] B. Wang, S. M. Anthony, S. C. Bae, and S. Granick, Proc. Natl. Acad. Sci. USA **106**, 15160 (2009).
[26] M. P. Lettinga, C. M. van Kats, and A. P. Philipse, Langmuir **16**, 6166 (2000).
[27] B. Wang, J. Kuo, S. C. Bae, and S. Granick, Nat. Mater. **11**, 481 (2012).
[28] J. Kim, C. Kim, and B. J. Sung, Phys. Rev. Lett. **110**, 047801 (2013).
[29] M. J. Skaug, J. Mabry, and D. K. Schwartz, Phys. Rev. Lett. **110**, 256101 (2013).
[30] S. Bhattacharya, D. K. Sharma, S. Saurabh, S. De, A. Sain, A. Nandi, and A. Chowdhury, J. Phys. Chem. B **117**, 7771 (2013).
[31] J. Guan, B. Wang, and S. Granick, ACS Nano **8**, 3331 (2014).
[32] T. Abete, A. de Candia, E. Del Gado, A. Fierro, and A. Coniglio, Phys. Rev. E **78**, 041404 (2008).
[33] R. Pramanik, T. Ito, and D. A. Higgins, J. Phys. Chem. C **117**, 3668 (2013).
[34] R. Pramanik, T. Ito, and D. A. Higgins, J. Phys. Chem. C **117**, 15438 (2013).
[35] C. Macias-Romero, M. E. P. Didier, V. Zubkovs, L. Delannoy, F. Dutto, A. Radenovic, and S. Roke, Nano Lett. **14**, 2552 (2014).
[36] G. P. Sinha and F. M. Aliev, Phys. Rev. E **58**, 2001 (1998).
[37] D. Kang, C. Rosenblatt, and F. M. Aliev, Phys. Rev. Lett. **79**, 4826 (1997).
[38] F. Höfling, T. Franosch, and E. Frey, Phys. Rev. Lett. **96**, 165901 (2006).
[39] F. Höfling, Ph.D. thesis, Ludwig-Maximilians-Universität München, 2006.
[40] F. Höfling, E. Frey, and T. Franosch, Phys. Rev. Lett. **101**, 120605 (2008).
[41] B. J. Sung and A. Yethiraj, Phys. Rev. Lett. **96**, 228103 (2006).
[42] B. J. Sung and A. Yethiraj, J. Phys. Chem. B **112**, 143 (2008).
[43] H. W. Cho, G. Kwon, B. J. Sung, and A. Yethiraj, Phys. Rev. Lett. **109**, 155901 (2012).

[44] J. Szymanski and M. Weiss, Phys. Rev. Lett. **103**, 038102 (2009).
[45] M. Weiss, Phys. Rev. E **88**, 010101(R) (2013).
[46] P. Massignan, C. Manzo, J. A. Torreno-Pina, M. F. García-Parajo, M. Lewenstein, and G. J. Lapeyre, Jr., Phys. Rev. Lett. **112**, 150603 (2014).
[47] N. Oppenheimer and H. Diamant, Phys. Rev. Lett. **107**, 258102 (2011).
[48] M. P. Allen and D. J. Tildesley, *Computer Simulation of Liquids* (Oxford University Press, New York, 1987).
[49] See Supplemental Material at http://link.aps.org/supplemental/10.1103/PhysRevE.90.042105 for additional simulation results for $g(\theta,t|D_R)$ and $U(t)$.
[50] A. Okabe, B. Boots, K. Sugihara, and S. N. Chiu, *Spatial Tessellations* (Wiley, New York, 2000).
[51] R. Zwanzig, *Nonequilibrium Statistical Mechanics* (Oxford University Press, New York, 2001).
[52] T. Ha, J. Glass, T. Enderle, D. S. Chemla, and S. Weiss, Phys. Rev. Lett. **80**, 2093 (1998).